HYBRID ZIGBEE-RFID NETWORKS WITH HIGHEST ENERGY EFFICIENCY

P. Medagliani[1], G. Ferrari[1], M. Marastoni[2]

[1] *Wireless Ad-hoc and Sensor Networks (WASN) Laboratory*
Department of Information Engineering
University of Parma
I-43100, Parma, Italy
[2] *Pride s.p.a.,*
I-20151, Milano, Italy

Abstract   Zigbee is the standard of choice in wireless personal area networks with low power consumption, such as, for example, sensor and control wireless networks. Since nodes may be positioned in non-easily accessible places, a high energy efficiency is required in order to maximize the network lifetime and minimize the maintenance costs. A simple and straightforward solution to maximize the network lifetime consists in turning off all nodes which are not needed, e.g., when the node spatial density is higher than that required to satisfy the sensing requirements. We propose an innovative radio-switched Zigbee network, where remote sensor nodes are selectively turned off. More precisely, the radio control is based on the use of Radio Frequency IDentification (RFID) technology, leading to a hybrid Zigbee/RFID architecture. In other words, we consider two logically overlapped networks, RFID and Zigbee. The RFID network turns on/off the nodes of the Zigbee network through a power-off algorithm, referred to as *deep sleep* algorithm, designed to equalize the residual energy in each Zigbee node. In fact, the RFID controller (i.e., the reader) cyclically switches off the Zigbee nodes with low amounts of residual energy. By building upon the proposed RFID-controlled Zigbee networks, we focus on applications which require a minimum *local* spatial density of observations. This is of interest, for instance, in distributed monitoring applications, where one needs to monitor the largest possible area in a homogeneous way. In this case, we introduce a *virtual spatial grid* over the monitored region, and we apply the deep sleep algorithm cell by cell of the grid, requiring that at most one node per cell is active at a time. The proposed hybrid Zigbee/RFID networks are analyzed through Opnet-based simulations.

Keywords: Zigbee, RFID, hybrid networks, energy efficiency, wireless sensor networks

1. INTRODUCTION

Wireless sensor networks are an interesting research topic, both in military [1–3] and civilian scenarios [7, 23]. In particular, remote/environmental monitoring, surveillance of reserved areas, etc., are important fields of application of wireless sensor networking techniques. These applications often require very low power consumption and low-cost hardware [18].

One of the newest standards for wireless networking with low transmission rate and high energy efficiency has been proposed by the Zigbee Alliance [12, 28]. An experimental analysis of Zigbee Wireless Sensor Networks (WSNs), taking into account the impact of the most important system parameters (e.g., the Received Signal Strength Indication (RSSI), throughput, network transmission rate, and delay) is presented in [10, 12, 17]. One of the most interesting research directions for WSNs is the design of network architectures with high energy efficiency. In [5], the authors analyze different approaches and possible optimization strategies in order to reduce the power consumption of IEEE 802.15.4 networks. In [22], instead, a mechanism for shutting down the radio frequency interface of wireless sensors, in order to reduce power consumption, is presented.

On the other side, Radio Frequency IDentification (RFID) devices are also receiving more and more attention, by both industrial and scientific communities. In particular, they can be used for luggage identification in airports, biological materials identification in hospitals, monitoring of post parcels, tracking of livestocks, efficient monitoring of objects in supply chains, etc. [11, 19, 25, 26]. One of the newest areas of interest for the RFID technology is pervasive computing, typically carried out integrating different technologies, such as RFID devices and WSNs [20]. In [24, 27], the authors propose and evaluate three different system architectures in order to combine WSNs with RFID systems.

We first introduce a logical scheme for the integration of Zigbee and RFID networks to maximize the battery lifetime of the nodes in the former network. Then, we analyze the performance of this integrated network in terms of energy consumption, considering a simple deep sleep algorithm, such that nodes are cyclically turned off once their battery energy becomes lower than a threshold level, which is adaptively adjusted during network evolution. Finally, in order to monitor the network surface uniformly, we introduce a virtual spatial grid and apply the deep sleep algorithm cell by cell of this grid.

The structure of this work is the following. In Section 2, a short overview on the Zigbee standard is provided, whereas in Section 3 we describe the RFID technology. In Subsection 4.1, we present the selective wake-up idea upon which our model is based, and in Subsection 4.2 the Opnet simulator structure of the integrated Zigbee-RFID network is presented. In Subsection 4.3, the im-

plementation of the deep sleep algorithm is considered and in Subsection 4.4 the concept of virtual spatial grid is presented. In Section 5, the performance of hybrid Zigbee-RFID networks is analyzed. Finally, Section 6 contains concluding remarks.

2.   ZIGBEE STANDARD OVERVIEW

The Zigbee standard is suited for the family of Low-Rate Wireless Personal Area Networks (LR-WPANs), allowing network creation, management, and data transmission over a wireless channel with the highest possible energy savings. Three different types of nodes are foreseen by the Zigbee standard: (i) *coordinator*, (ii) *router*, and (iii) *end device*. In the absence of a direct communication link, the router is employed to relay the packets towards the correct destination. The coordinator, in addition to relaying the packets, can also create the network, exchange the parameters used by the other nodes to communicate (e.g., a network IDentifier (ID), a synchronization frame, etc.), and send network management commands. The router and coordinator are referred to as *Full Function Devices* (FFDs), i.e., they can implement all the functions required by the Zigbee standard in order to set up and maintain communications. The end devices, which are also referred to as *Reduced Function Devices* (RFDs), can only collect data from sensors, insert these values into proper packets, and send them to destination nodes.

The Zigbee standard is based, at the first two layers of the ISO/OSI stack, on the IEEE 802.15.4 standard [14], which employs a *non-persistent* Carrier Sense Multiple Access with Collision Avoidance (CSMA/CA) Medium Access Control (MAC) protocol and operates in the 2.4 GHz band (similarly to the IEEE 802.11 standard [13]). In addition, the IEEE 802.15.4 standard provides an optional ACK message to confirm the correct delivery of a packet. We remark that the medium access mechanism in Zigbee wireless networks makes use of a *back-off algorithm* to reduce the number of packet collisions. A node, before transmitting a new packet, waits for a period whose length is randomly chosen within an interval defined during the network start-up phase. After this period of time has elapsed, the node tries to send its packet: if it detects a collision, it doubles the previously chosen interval and waits; if the channel is free, instead, it transmits its packet. This procedure is repeated for five times, after which the waiting interval is kept fixed to its maximum value. This back-off algorithm makes it likely, in the considered scenarios (low traffic load), that a node will eventually manage to transmit its packet.

The Zigbee standard provides a technique which improves the synchronization between RFDs. This technique is based on the subdivision of the time into *slots* and the transmission of a periodic signal, referred to as *beacon*, from the coordinator of the network. In particular, the standard defines a specific frame
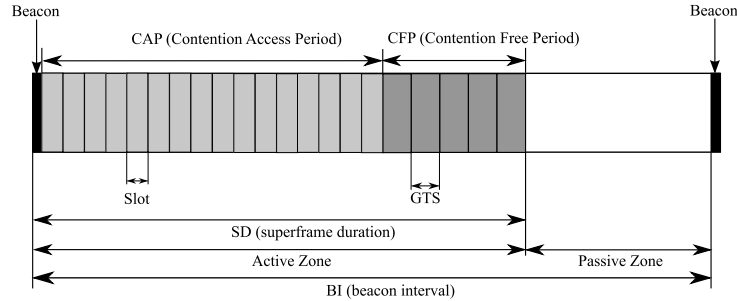
Figure 1. Structure of the superframe used by the Zigbee standard.

structure, referred to as *superframe*, shown in Figure 1. This frame is divided into two main zones: (i) active and (ii) passive. The active zone is divided, in turns, into two periods: (i) the Contention Access Period (CAP) and (ii) the Contention Free Period (CFP). In the CAP, the RFDs access the channel according to the CSMA/CA protocol, whereas in the CFP only the RFDs that have previously reserved a Guaranteed Time Slot (GTS) can access the channel, thus preveventing the collisions. Finally, in the passive zone all the RFDs switch into *sleep* state in order to improve the energy saving. [1] According to the Zigbee notation, the time interval between two subsequent beacons is referred to as Beacon Order (BO), whereas the duration of the active frame is referred to as Superframe Duration (SD).

3. RFID TECHNOLOGY

The RFID technology specifies two different devices: (i) the *reader* and (ii) the *transponder* or *tag*. The tag is an electronic device that stores data useful for identification and is placed on the object to be tracked. On the opposite, the reader is the device used to interrogate the tags. The tags can be classified into three main categories, according to the power source they are equipped with: (i) *active*, (ii) *semi-passive*, and (iii) *passive* [11]. The active tags, in order to respond to the interrogation of the reader, use their own internal batteries for processing operations and signal transmission. The semi-passive tags, instead, use their batteries only to power the internal processor and not to broadcast the return signal. Finally, the passive tags, being not equipped with batteries, exploit the energy of the received signal to respond to the reader (*backscattering* technique). Obviously, the tags with longer lifetime (virtually infinite) are the passive ones, whereas the active tags have the longest transmission range. Once the reader has interrogated a tag and this has replied correctly without incurring into collisions with other tags (proper anti-collision mechanisms are

used [6]), the reader sends an *acknowledgment* message to the tag to confirm correct message reception.

The functionalities provided by the RFID technology are mainly related to error-free communication between reader and tags (bidirectional), identification and communication with multiple tags, selection of a target set of tags, lock of data stored in the tags, and writing and overwriting operations in the tags. The communication from the reader to the tags, according to the backscattering technique, is realized through amplitude modulation of the interrogation signal. On the other hand, after the transmission of the interrogation signal, the reader emits a constant-power signal which allows the tags to respond to the former signal through a load modulation technique [11]. The reader receives data from the tags as a variation of the reflection of the constant-power signal.

When the reader interrogates a set of tags, these may respond immediately, leading to a collision. One of the most important standards for the RFID technology is the ISO/IEC 18000-6 standard [15]. This standard defines a reference model for identification systems which operate in the range of Ultra High Frequencies (UHF). In particular, this standard regulates RFID systems in the frequency band around 868 MHz in Europe. The 18000-6 standard defines two different transmission types: (i) *type A* and (ii) *type B*. Both transmission types make use of a rate equal to 40 kbps and use a binary phase modulation. The difference between these two transmission types resides in the medium access control (MAC) protocol. If a collision is detected by the reader, the Type A tags retransmit the interrogation request according to the *Aloha* MAC protocol [4]. According to this protocol, a tag transmits as soon as a packet is generated and it assumes that a collision has happened if an acknowledgment message is not received after a given period of time. Type B tags, instead, use the Binary Tree Protocol (BTP) [6] as anti-collision mechanism. The idea of the BTP is that, upon a collision, the set of tags is divided into two subsets: one set tries to retransmit their messages immediately, whereas the other set waits till a new interrogation request is generated by the reader. Eventually, only one tag will retransmit, and its identity (or any other stored information) will be successfully acquired by the reader. This recursive procedure is then repeated, under the constraint that the already censed tags do not respond to the interrogation signal.

## 4.	HYBRID ZIGBEE-RFID NETWORKS

### 4.1	System Model

Our system model consists of a network where *N* nodes are deployed to monitor a particular phenomenon of interest. Under the assumption that a min-
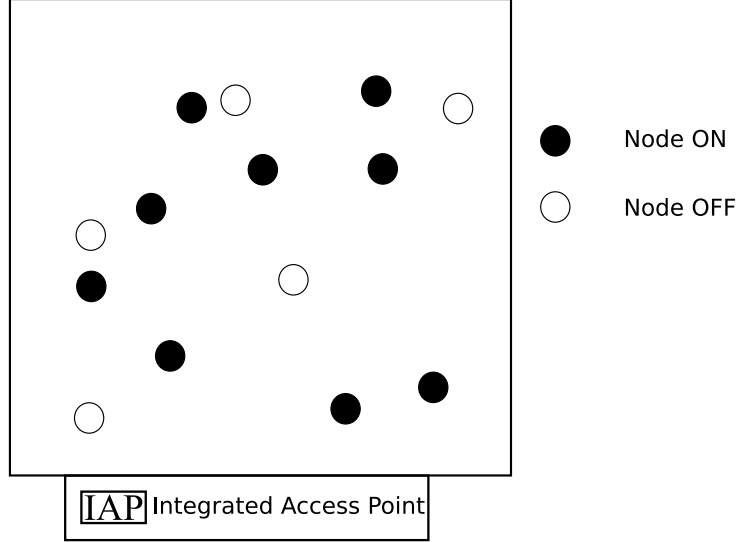
Figure 2. Network scenario with $N = 14$ nodes, out of which and $N_{\min} = 9$ are active and $N - N_{\min} = 5$ have been turned off by the deep sleep algorithm.

imum spatial density of observations is required, i.e., a minimum number $N_{\min}$ of RFDs needs to be used to monitor a given surface (with area A) of interest, and that the number N of deployed RFDs is larger than $N_{\min}$, our approach consists in implementing a *selective wake-up* of the RFDs. More precisely, our strategy consists in selectively turning on and off the RFDs in order to equalize the energy consumption of the nodes in the network. In order to maximize the network lifetime, as soon as the residual energy of an active RFD becomes lower than a fixed threshold E_{th}, the RFD is switched into the sleep state. At the same time, one of the remaining $N - N_{\min}$ RFDs (previously switched off) is woken up, so that an overall minimum spatial density of observations of the phenomenon of interest is guaranteed. This procedure is referred to as *deep sleep algorithm.* An illustrative example of the status, at a given time, of a network where the deep sleep algorithm is used, is shown in Figure 2. We point out that the RFDs are only switched into the sleep state, instead of being turned off, in order to prevent them from losing synchronization with the coordinator and the other RFDs in the network. In fact, according to the Zigbee standard, the network joining operations performed when an RFD is turned on introduce a delay longer than the length of the wake up operations, since the RFD must wait for a new beacon in order to synchronize with the network before starting its transmission. On the opposite, the RFDs in the sleep state switch to the active state only when a beacon transmission is scheduled and subsequently,

if not required, return into the sleep state without losing their synchronization with the network. The goal of the deep sleep algorithm is energy equalization among the RFDs, so that the residual energies of the RFDs are balanced. When an RFD is in the sleep state, in fact, its energy consumption is four orders of magnitude lower than in the active state [8, 16].

4.2   Opnet Simulator Structure

Our hybrid Zigbee-RFID model is based on an IEEE 802.15.4 Opnet model developed at the University of Porto, Portugal [21] and on an RFID Opnet model developed at the University of Parma, Italy [9]. The IEEE 802.15.4 model is beaconed in order to synchronize the nodes in the network and save energy. In addition, this model contains a battery module which is used to evaluate the energy consumption of the devices.[2] On the other side, the Opnet RFID model implements the ISO/IEC 18000-6 standard, considering faded wireless channels. Since the Zigbee and RFID models are disjoint, we have developed a hybrid Opnet Zigbee-RFID model where the subcomponents communicate and cooperate.[3] Obviously, the beaconing mechanism is modified in order to take into account also the RFDs which are not transmitting during a frame. Note that in our system the BTP (embedded in the ISO/IEC 18000-6 standard) is not used, since the RFID tags are used only as switches for the (Zigbee) RFDs and do not need to be identified. In Figure 3 (a), the logical scheme of the integrated Zigbee-RFID network is shown. More precisely, the RFID network lays on top of the Zigbee network. In our hybrid system, the information is transferred through the IEEE 802.15.4 (logical) network which is, in turn, controlled by the RFID network. In Figure 3 (b), instead, we show the integrated devices used in our network: the *integrated AP*, which is obtained from the combination of an RFID reader and a Zigbee coordinator; and *integrated node*, which is obtained from the combination of an RFID tag and a Zigbee RFD. We point out that the integrated node is battery powered, whereas the integrated AP is supposed to be connected to the electrical system, so that battery exhaustion is not an issue for the latter, but only for the former.

4.3   Deep Sleep Algorithm

We now describe the basic functionalities of an hybrid Zigbee-RFID network. When an RFD is in the sleep state and is selected by the coordinator, the associated RFID tag receives the signalling message from the reader (through the logical RFID network) and switches on its RFD, which enters into the active state and starts communicating (through the logical Zigbee network). Similarly, when an RFD is active and its residual energy becomes lower than a threshold value, the RFD communicates it to the Zigbee coordinator. The
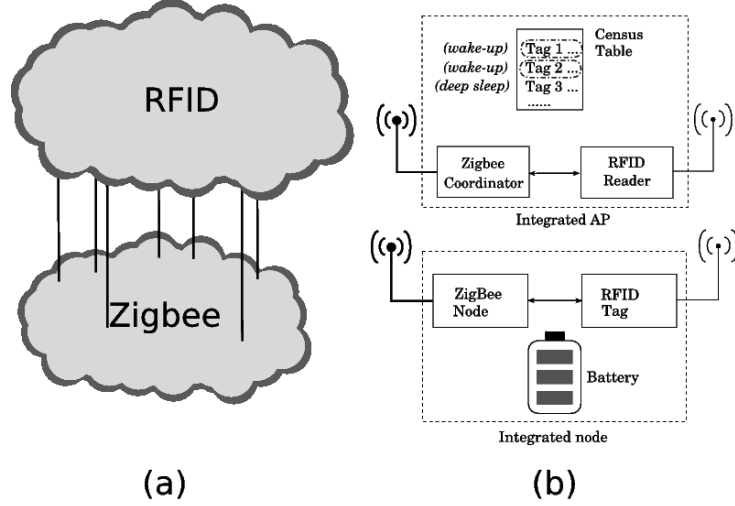
Figure 3. Logical scheme of the integrated network: (a) the Zigbee and RFID networks are combined together; (b) the integrated nodes and AP are obtained from the integration of Zigbee and RFID devices.

coordinator informs its associated RFID reader, which, by sending a proper message to the tag, forces the selected RFD into the sleep state. Since the deep sleep algorithm is managed by the coordinator of the Zigbee network, the active RFDs embed their residual energies inside the data packets sent to the coordinator. In this way, the coordinator is constantly aware of the residual energy of each active RFD. On the other hand, since an RFD in the sleep state does not transmit any packet, the coordinator also uses an estimation algorithm to predict the energy consumed by an RFD during the sleep state.

We now describe the main steps of the deep sleep algorithm through illustrative diagrams. Figure 4 refers to the operations involved when the network is started. All the RFDs are equipped with identical batteries and we refer to the initial energy level as 100%. At the network start-up, only N_{min} RFDs are turned on, whereas the remaining $N - N_{min}$ nodes are turned into the sleep state. The integrated AP creates a *census table*, where information about the position, the residual energy, and the status of each RFD is stored. In our simulations, we assume that the position of each RFD is preliminarily available at the integrated AP, whereas the entry of the census table relative to the residual energy of an RFD is updated as soon as a packet (containing this information) is received from the node. If an RFD is in the sleep state, its residual energy value is estimated by the AP before scheduling the transmission of a new beacon.
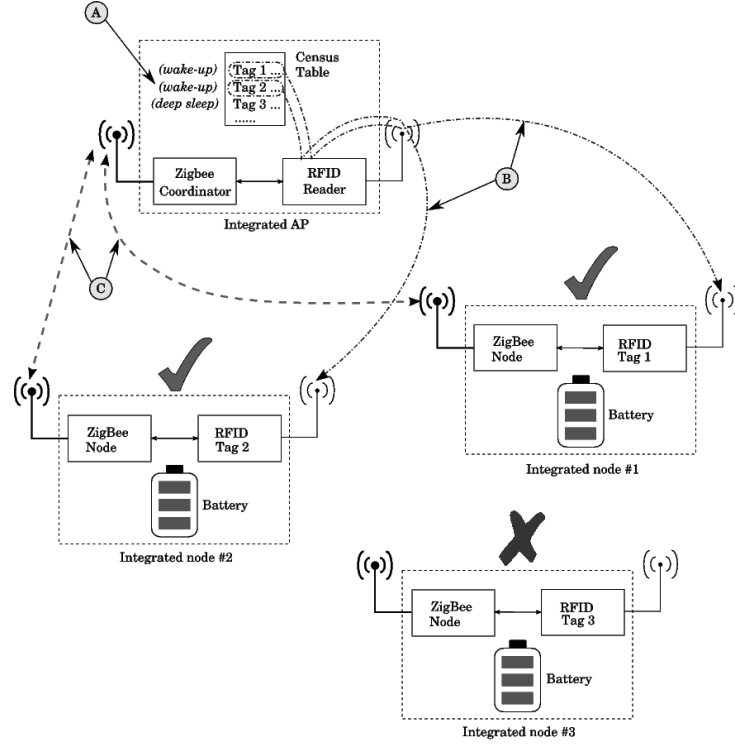
Figure 4. Initial steps of the deep sleep algorithm for selective wake-up of remote nodes: (A) $N_{\min}$ out of N RFDs are selected by the AP; (B) the selected RFDs are notified through the associated RFID tags; (C) the activated RFDs start communicating.

As soon as an RFD is turned on, its residual energy E_r reduces and, consequently, its value in the census table is updated. The evolution of the network according to the deep sleep algorithm is illustrated in Figure 5. When the energy of an RFD becomes lower than an initial threshold $E_{th}^{(0)}$, the integrated AP forces the RFD into the sleep state through its associated RFID tag. At the same time, the integrated AP forces one of the sleeping nodes with higher residual energy to wake up. This procedure is repeated until there are no more RFDs with residual energies higher than $E_{th}^{(0)}$. At this point, the threshold value of the residual energy is decreased of a pre-defined energy step E_s. More precisely, the new energy threshold is set to $E_{th}^{(1)} = E_{th}^{(0)} - E_s$. This procedure is repeated until the energy threshold is so low that data communications in the Zigbee logical network are no longer possible.[4] At this point, as soon as the minimum spatial density of observations is no longer guaranteed, the network is declared
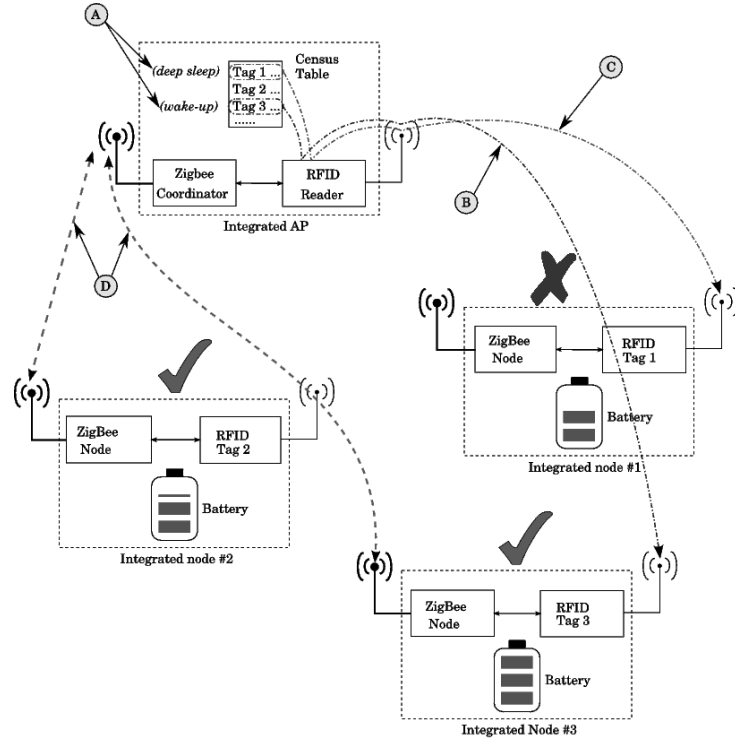
Figure 5. Steps of the replacement of an active node with residual energy under threshold and a sleeping node with higher residual energy: (A) the AP identifies an RFD with low residual energy; (B) a sleeping node with high residual energy is turned on and (C) the selected active RFD with low residual energy is turned off; (D) the set of active nodes communicate.

dead and the simulation stops. More details on the energy consumption at the nodes will be given in Subsection 5.1.

In general, N integrated nodes could be deployed randomly over a given surface. As an illustrative scenario, in Figure 6 $N = 27$ nodes are deployed randomly over a square surface. The integrated AP is placed in the center of the monitored surface, whereas the $N = 27$ integrated nodes are deployed according to a 2-D Poisson distribution.

4.4 Deep Sleep Algorithm with Virtual Spatial Grid

While the deep sleep algorithm takes into account the *overall* observation spatial density (considering the total number of nodes deployed over the entire network surface), in several applications it might be of interest to monitor *homogeneously* the network surface, i.e., to guarantee an approximately constant
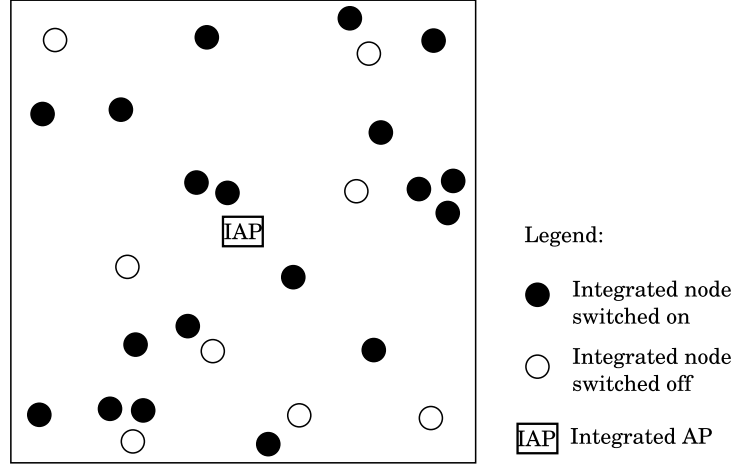
Figure 6. Network scenario with $N = 27$ nodes, out of which and $N_{\min} = 19$ are active and $N - N_{\min} = 8$ have been turned off by the deep sleep algorithm. The monitored surface is not divided into cells..

local observation spatial density across the surface. In order to do this, we follow an approach based on the use of a *virtual spatial grid* over the network.

If the monitored area is virtually partitioned into observation cells (with a local minimum required node spatial density per cell), then the "standard" deep sleep algorithm can no longer be applied, since it could lead to turn off all nodes of the same cell. However, there might be scenarios where particularly critical phenomena need to be observed with high accuracy over the entire monitored surface. In Figure 7, an illustrative example of the network in Figure 6 with an overlaid virtual spatial grid is shown. As one can see, different cells may contain different numbers of nodes. In the following, we will denote the cells where there is only one integrated node as *secondary*, whereas the cells with more than one integrated node will be denoted as *primary*. In the presence of a virtual spatial grid, the deep sleep algorithm is applied in each primary cell, where the observations are redundant. In the secondary cells, no deep sleep algorithm is applied, since the integrated nodes cannot be turned off. The cells with no node are not relevant for monitoring purposes.

The network is declared dead as soon as all the RFDs of one of the primary cells die. This criterion comes from the assumption that primary cells are assumed to be associated with critical zones of the phenomenon under observation, whereas the secondary cells may be associated with less critical zones. Thus, when a primary cell contains no more RFD, we assume that the observations are no longer reliable and the network is declared dead. We remark that
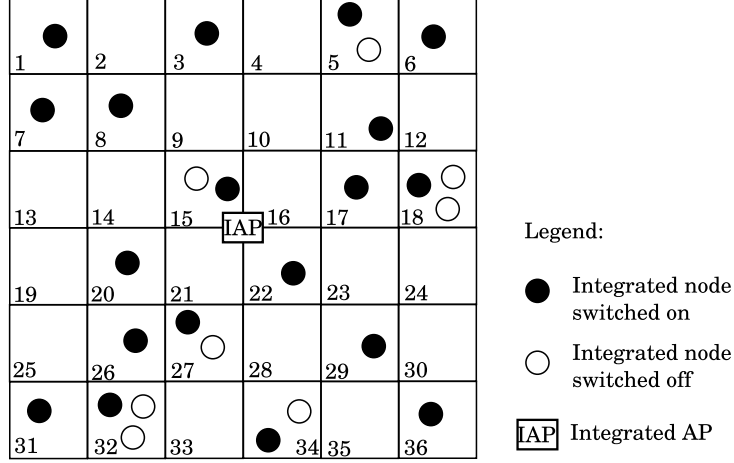
Figure 7. Network scenario with $N = 27$ nodes, out of which and $N_{min} = 19$ are active and $N - N_{min} = 8$ have been turned off by the deep sleep algorithm. The monitored surface is divided into cells and only one node per cell is active, according to the spatial grid procedure.

our approach is valid also in scenarios where $N > N_{min}$, but it is more effective in scenarios where $N \gg N_{min}$.

5. PERFORMANCE ANALYSIS

The simulations have been carried out considering networks with $N = 40$ nodes deployed over a square surface with 6 m long sides. In all cases, the RFDs send packets directly to the integrated AP, i.e., all network realizations have star topologies. The packet interarrival time T_{int} is either fixed to 0.25 s or Poisson-distributed with average value equal to 0.25 s. The considered packet length is $L = 200$ bit/pck. We assume that the network is dead when the energy level of all RFDs becomes 80% of the initial value. Each performance simulation result is the average of the results obtained considering 6 realizations of the network topology (according to a 2-D Poisson distribution).

Before starting the simulation-based performance analysis of hybrid Zigbee-RFID networks using the deep sleep algorithm, we provide the reader with some details about the energy consumed by each integrated node. The average residual energy[5] at a generic instant t can be expressed as follows:

$$E_r(t) = E_i - E_c(t) \tag{1.1}$$

where E_i is the initial energy of a node and $E_c(t)$ is the energy consumed at the instant t. In particular,

$$E_c(t) = E_{c\_TX}(t) + E_{c\_RX}(t) + E_{c\_idle}(t) + E_{c\_sleep}(t)$$

where:

$$
\begin{aligned}
E_{\text{c\_TX}}(t) &= \lambda \cdot E_{\text{c\_TX\_1\_pck}} \cdot t = K_{\text{TX}} \cdot t \\
E_{\text{c\_RX}}(t) &= \lambda \cdot (N-1) \cdot E_{\text{c\_RX\_1\_pck}} \cdot t = K_{\text{RX}} \cdot t \\
E_{\text{c\_sleep}}(t) &\simeq E_{\text{c\_sleep\_1\_s}} \cdot \frac{\Delta t_{\text{passivezone}}}{\Delta t_{\text{superframe}}} \cdot t = K_{\text{sleep}} \cdot t \\
E_{\text{c\_idle}}(t) &\simeq E_{\text{c\_idle\_1\_s}} \cdot \frac{\Delta t_{\text{activezone}}}{\Delta t_{\text{superframe}}} \cdot \\
&\quad \cdot \left[t - \Delta t_{\text{TX\_1\_pck}} \cdot \lambda \cdot t - \Delta t_{\text{RX\_1\_pck}} \cdot \lambda \cdot (N-1) \cdot t \right] \\
&= K_{\text{idle}} \cdot t
\end{aligned}
$$

λ is the packet transmission rate[6]; $E_{\text{c\_TX\_1\_pck}}$ and $E_{\text{c\_RX\_1\_pck}}$ are the energies consumed per packet transmission and reception acts, respectively; $E_{\text{c\_sleep\_1\_s}}$ and $E_{\text{c\_idle\_1\_s}}$ are the energies consumed during one second of persistence in the sleep and idle states, respectively; and $\Delta t_{\text{activezone}}$, $\Delta t_{\text{passivezone}}$, and $\Delta t_{\text{superframe}}$ are the durations of the active zone, the passive zone, and the superframe, respectively. Therefore, we can approximate $E_{\text{c}}(t)$ as

$$
E_{\text{c}}(t) \simeq \left[K_{\text{TX}} + K_{\text{RX}} + K_{\text{sleep}} + K_{\text{idle}} \right] \cdot t = K_{\text{tot}} \cdot t \tag{1.2}
$$

Using (1.2) into (1.1), the residual energy at time t can be rewritten as

$$
E_{\text{r}}(t) \simeq E_{\text{i}} - K_{\text{tot}} \cdot t . \tag{1.3}
$$

The final expression (1.3) for the residual energy is obtained under the assumption of no use of the deep sleep algorithm. However, if the deep sleep algorithm is used, only the values of K_{sleep} and K_{idle} change, but the linear dependence of E_{r} from t still holds, as will be shown in the following.

5.1   Deep Sleep Algorithm

In Figure 8, we evaluate the impact of the energy step E_{s} on the average (over the integrated nodes) residual energy in three different scenarios, considering $N = 40$ nodes in all cases: (i) with $N_{\text{min}} = 40$ (i.e., the deep sleep algorithm is not used), (ii) with $N_{\text{min}} = 30$, and (iii) with $N_{\text{min}} = 25$. The packet generation rate is constant where packet interarrival time equal to 0.25 s is used. Observing the curves related to the scenarios with the deep sleep algorithm, it can be noted that the performance for a given value of N_{min} does not depend on E_{s}. This is to be expected, provided that the energy step is sufficiently smaller than the initial energy. In fact, when the deep sleep algorithm is used, N_{min} nodes are active at a time, and the value of E_{s} determines only the rate at which nodes get activated and deactivated. In particular, the following considerations can be carried out.
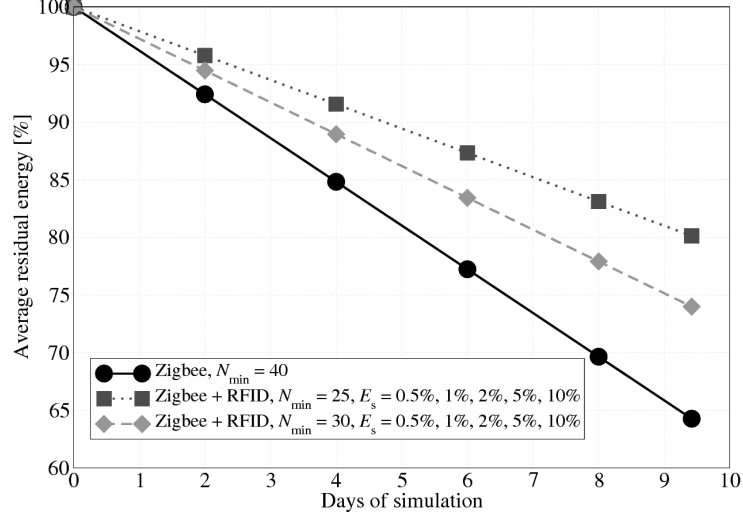
Figure 8. Average residual energy as a function of the days of simulation, in scenario with $N = 40$ nodes. Various values (25, 30, 40) of N_{min} are considered for the application of the deep sleep algorithm. In the case with $N_{min} < N$, various values of the energy step are used.

- If E_s is very small, then the energy levels of the nodes are equalized in a very fine way. However, this implies that nodes will cycle between on and off states very often, i.e., the integrated AP will spend energy in sending control messages and in the processing required to track the network topology changes.

- On the other hand, if E_s is not too small, then energy equalization is "rougher" but the integrated AP will spend less energy in network management operations. Since energy consumption is typically not an issue for the integrated AP, "finer" energy equalization should be chosen.

To summarize, the network behavior of a hybrid Zigbee-RFID network using the deep sleep algorithm is very similar to a "standard" Zigbee network with N_{min} RFDs, regardless of the value of E_s.

In Figure 9, the average residual energy is shown as a function of the number of days of simulation, for various values of the number N_{min} of active RFDs. We have considered only $E_s = 1\%$ because, as shown in Figure 8, the average residual energy is independent of E_s. Observing the curves in Figure 9, one can conclude that:

- the smaller N_{min}, the higher the energy saving, regardless of the simulation duration;
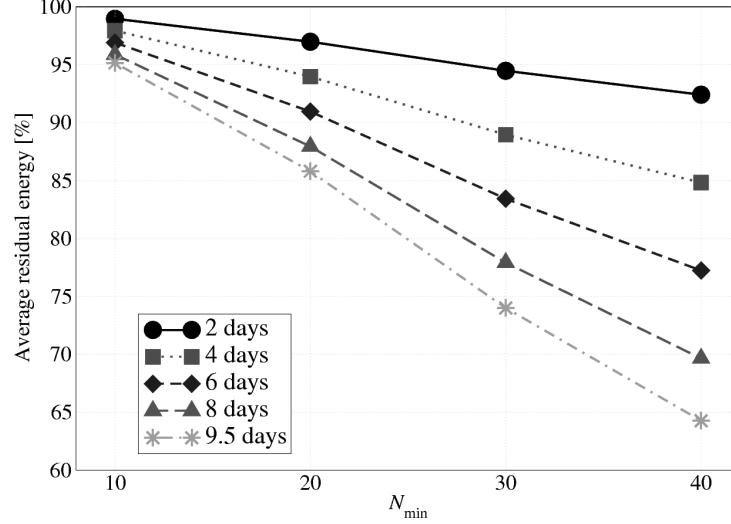
Figure 9. Average residual energy, as a function of $N_{\min}$, considering various values for the number of days of simulation. In all cases, $N = 40$.

■ the performance of the network without the deep sleep algorithm (i.e., the scenario with $N_{\min} = 40$) is the worst.

According to the deep sleep algorithm, in fact, when $N_{\min}$ is small, there is a large number of RFDs in the sleep state, and the energy consumption (averaged over all RFDs in the network) is, therefore, low. On the opposite, when $N_{\min}$ is large or, as a limiting case, the deep sleep algorithm is not used ($N = N_{\min}$), there is a large number of RFDs active in the network, and the energy consumption is high.

In Figure 10, the average residual energy is shown as a function of the number of days of simulations, considering constant and Poisson packet generation distributions. As mentioned at the beginning of this section, the packet generation rate is $\lambda = 4$ pck/s—this is the *average* packet generation rate with Poisson distribution. As one can see from results in Figure 10, the average residual energy is a linearly decreasing function of the time *regardless* of the packet generation distribution. However, for a given value of $N_{\min}$, it can be observed that a Poisson distributed packet generation leads to a performance degradation with respect to the case with constant packet generation, and this degradation is more pronounced the larger is $N_{\min}$. This is due to the higher traffic generated with the Poisson distribution. Each active node receives all the packets transmitted in the network and processes only those with a destination address equal to its own address. On the other hand, when a node is in the sleep state, no packet is received and energy is preserved.
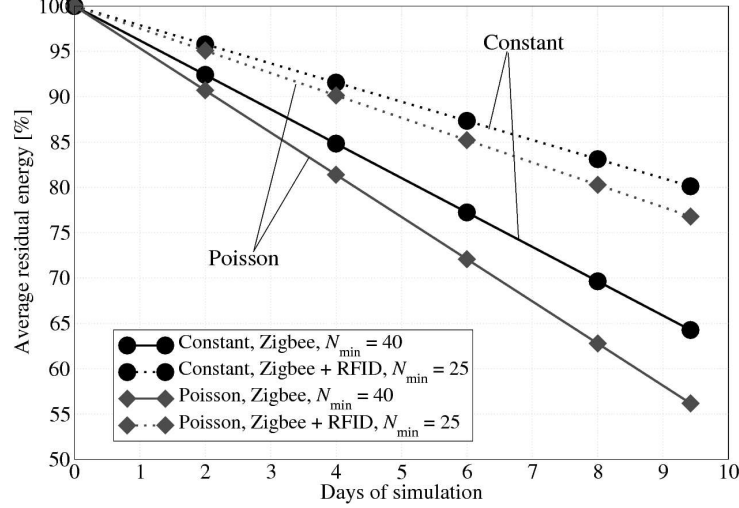
Figure 10. Average residual energy, as a function of the number of days of simulation, for various packet generation distributions: (i) constant and (ii) Poisson. In all cases, $N = 40$, whereas N_{min} is set to either 25 or 40.

Finally, we point out that, also with Poisson-distributed packet generation, different values of the energy step E_{s} do not influence the observed performance.

5.2 Impact of the Virtual Spatial Grid

In this section, we present performance results in scenarios where a virtual spatial grid is considered and the deep sleep algorithm is applied locally, as described in Subsection 4.4. The same network topology of Subsection 5.1 is considered and the monitored surface is divided into 36 1 m² cells. We remark that, according to our algorithm, in the secondary cells the nodes are turned on according to the traditional superframe structure. In the primary cells, where the deep sleep algorithm is applied cell by cell, instead, there is at least one active node per cell, whereas the other nodes of the cell are cyclically switched into the sleep state.

We have considered different network configurations and we have compared the results in the presence of the virtual spatial grid with those of scenarios without it. For different types of networks, we have considered the same network topology realizations, in order to make the comparison fair.

In Figure 11, we present the average number of active cells guaranteed by the two different node management mechanisms. On average, using the different topologies considered in our simulation framework, the virtual spatial
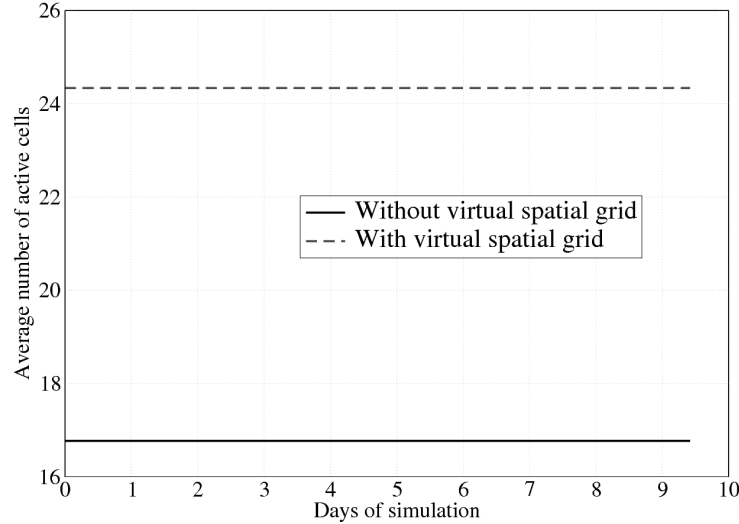
Figure 11.   Average cells coverage with and without the virtual spatial grid. In all cases, the deep sleep algorithm is used ($N_{min} = 25$) and $N = 40$.

grid procedure guarantees the coverage of 24 cells, whereas a scenario without virtual spatial grid procedure leads to an average of 17 active cells. As one can see, the average number of active cells remains constant over the simulation: this is due to the fact that in both cases the battery energy is not depleted.

In Figure 12 the average energy consumption performance is shown as a function of the number of simulation days, considering scenarios without the deep sleep algorithm ($N_{min} = 40$), with the deep sleep algorithm without virtual spatial grid ($N_{min} = 20$, or $N_{min} = 25$), and with the virtual spatial grid. The curves presented in this figure are obtained in a scenario with $E_s = 1\%$, because we have experienced that, as in the case with deep sleep algorithm, the energy step has no impact on the performance of networks with the virtual spatial grid. The energy consumption of a traditional Zigbee network is larger than that of networks with deep sleep algorithm both with and without virtual spatial grid. In particular, in scenarios where the virtual spatial grid is applied, on average there are 24 active nodes, and the average residual energy trend is similar to that of the network with deep sleep algorithm and without virtual spatial grid with $N_{min} = 25$.

6.   CONCLUSIONS

We have proposed an approach to integrate Zigbee and RFID networks in order to create an energy-efficient network which allows to selectively turn on
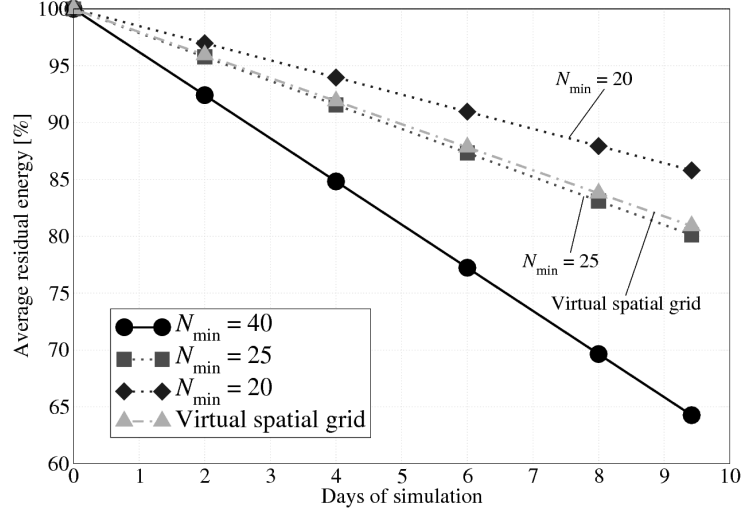
Figure 12. Average energy consumption with energy step equal to 1% of the initial energy level. The number of nodes is $N = 40$. The deep sleep algorithm is applied considering $N_{min} = 20$, $N_{min} = 25$, respectively. The performance with the virtual spatial grid is also shown.

and off the remote nodes. Therefore, we have proposed a deep sleep algorithm which selects the nodes to be activated according to their residual energy, so that the energy consumption of the nodes in the network is equalized. Finally, we have introduced a procedure which selects the integrated nodes to be activated according not only to their residual energy, but also to their spatial positions. This selection is based on the introduction of a virtual spatial grid over the network surface, and *local* application of the deep sleep algorithm. For the configurations without virtual spatial grid, we have evaluated through the Opnet simulator the average residual energy performance as a function of N_{min}, E_s, highlighting the energy saving guaranteed by the hybrid Zigbee-RFID network. For the configurations with virtual spatial grid, instead, we have analyzed both the area effectively monitored by the sensor network and the energy consumption. In this case, the virtual spatial grid not only provides the same area coverage than traditional Zigbee networks, but also allows to extend the network lifetime. This solution, which should be applied in scenarios where local observation spatial density is relevant, could be adopted in order to create a very energy-efficient wireless sensor network based on totally passive components with addressing capabilities.

NOTES

1. We remark that the energy consumption in the active periods is three orders of magnitude higher than that in the passive periods.

2. We remark that the energy consumption values considered in this model are typical of MICAz devices [8].

3. We point out that the realization of an experimental prototype physically connecting a Zigbee RFD with an RFID tag is currently under study.

4. Denoting by n_{fin} the final updating step, $E_{\text{th}}^{(n_{\text{fin}})} = E_{\text{th}}^{(0)} - n_{\text{fin}} \cdot E_{\text{s}}$ is too low to support communication in the Zigbee network. The value of n_{fin} depends on the specific parameters of the Zigbee network.

5. The residual energy $E_{\text{r}}(t)$ is the exact, not only the average, residual energy in the case of Poisson-distributed packet generation.

6. In the case of constant packet interarrival time T_{int}, $\lambda = 1/T_{\text{int}} = 4$ pck/s, whereas in the case of Poisson-distributed packet generation, $\lambda = 4$ pck/s is the *average* packet transmission rate.

REFERENCES

[1] Abileah, R., Lewis, D.: Monitoring high-seas fisheries with long-range passive acoustic sensors. In: Proc. Int. Conf. OCEANS'96: Prospects for the 21th century. Volume 1., Fort Lauderdale, FL, USA (1996) 378–382

[2] Akyildiz, I.F., Su, W., Sankarasubramaniam, Y., Cayirci, E.: A survey on sensor networks. IEEE Commun. Mag. **40** (2002) 102–114

[3] Barberis, S., Gaiani, E., Melis, B., Romano, G.: Performance evaluation in a large environment for the AWACS system. In: Proc. Int. Conf. on Universal Personal Communications (ICUPC'98). Volume 1., Florence, Italy (1998) 721–725

[4] Bertsekas, D., Gallagher, R.: Data Networks. Prentice-Hall, Upper Saddle River, NJ, USA (1992)

[5] Bougard, B., Catthoor, F., Daly, D.C., Chandrakasan, A., Dehaene, W.: Energy Efficiency of the IEEE 802.15.4 Standard in Dense Wireless Microsensor Networks: Modeling and Improvement Perspectives. In: Proc. in Design, Automation and Test in Europe (DATE'05), Munich, Germany (2005) 196–201

[6] Capetanakis, J.: Tree algorithms for packet broadcast channels. IEEE Trans. on Information Theory **25** (1979) 505 – 515

[7] Chong, C.Y., Kumar, S.P.: Sensor networks: evolution, challenges, and opportunities. Proc. IEEE **91** (2003) 1247–1256

[8] Crossbow Technology, Inc.: MICAz OEM Module 2.4GHz, San Jose, CA, USA. (2005) Datasheet, website: `http://www.xbow.com/Products/productdetails.aspx?sid=191`.

[9] Ferrari, G., Cappelletti, F., Raheli, R.: A simple performance analysis of RFID networks with binary tree collision arbitration. International Journal on Sensor Networks **4** (2008) 61–75

[10] Ferrari, G., Medagliani, P., Di Piazza, S., Martalò, M.: Wireless sensor networks: Performance analysis in indoor scenarios. EURASIP J. Wireless Commun. and Networking (2007) (To appear).

[11] Finkenzeller, K.: RFID Handbook - Fundamentals and Applications in Contactless Smart Cards and Identification. John Wiley & Sons, New York, NY, USA (2003)

[12] Hyncica, O., Kacz, P., Fiedler, P., Bradac, Z., Kucera, P., Vrba, R.: The Zigbee experience. In: Proc. Int. Symposium on Communications, Control and Signal Processing (ISCCSP'06), Marrakech, Morocco (2006)

[13] IEEE 802.11 Std: Wireless LAN Medium Access Control (MAC) a Physical Layer (PHY) specifications. IEEE Computer Society Press (1997) 1–459

[14] IEEE 802.15.4 Std: Wireless Medium Access Control (MAC) and Physical Layer (PHY) Specifications for Low-Rate Wireless Personal Area Networks (LR-WPANs). IEEE Computer Society Press (2003) 1–679

[15] ISO/IEC 18000-6: Information Technology – Radio Frequency Identification for Item Management – Part 6: Parameters for Air Interface Communications at 860 MHz to 960 MHz. International Organization for Standardization (ISO) (2004) 1–134

[16] Jurcik, P., Koubaa, A.: The IEEE 802.15.4 OPNET simulation model: reference guide v2.0. Technical report, IPP HURRAY! Research Group, Polytechnic Institute of Porto (ISEP-IPP), Porto, Portogallo (2007) website: http://www.open-zb.net/research.php.

[17] Lee, J.S.: An experiment on performance study of IEEE 802.15.4 wireless networks. In: In Proc. 10th Conference on Emerging Technologies and Factory Automation 2005, (ETFA'05). Volume 2., Catania, Italy (2005) 451–458

[18] Madou, M.: Fundamentals of Microfabrication. CRC Press (1997)

[19] Nath, B., Reynolds, F., Want, R.: RFID Technology and Applications. IEEE Pervasive Computing **5** (2006) 22–24

[20] Ni, L.M., Liu, Y., Lau, Y.C., Patil, A.P.: LANDMARC: indoor location sensing using active RFID. Pervasive Computing and Communications, 2003. (PerCom 2003). Proc. of the First IEEE Int. Conf. (2003) 407 – 415

[21] Polytechnic Institute of Porto, IPP-HURRAY! Research Group: (http://www.hurray.isep.ipp.pt:8080/opnet.html)

[22] Ramachandran, I., Das, A.K., Roy, S.: Analysis of the Contention Access Period of IEEE 802.15.4 MAC. ACM Trans on Sensor Networks (TOSN) **3** (2007) 1–29

[23] Simic, S.N., Sastry, S.: Distributed environmental monitoring using random sensor networks. In: Proc. 2-nd Int. Work. on Inform. Processing in Sensor Networks, Palo Alto, CA, USA (2003) 582–592

[24] Sung, J., Sanchez Lopez, T., Kim, D.: The EPC Sensor Network for RFID and WSN Integration Infrastructure. Pervasive Computing and Communications Workshops, 2007. (PerCom Workshops '07). Fifth Annual IEEE Int. Conf. (2007) 618 – 621

[25] Vogt, H.: Efficient Object Identification with Passive RFID Tags. In: Proc. of the 1st Int. Conf. on Pervasive Computing (PERVASIVE'03), Denver, CO, USA (2002) 98–113

[26] Weinstein, R.: RFID: a Technical Overview and its Application to the Enterprise. IT Professional **7** (2005) 27–33

[27] Zhang, L., Wang, Z.: Integration of RFID into Wireless Sensor Networks: Architectures, Opportunities and Challenging Problems. In: Proc. of 5th Int. Conf. on Grid and Cooperative Computing Workshops (GCCW'06), Changsha, Hunan, China (2006) 463–469

[28] Zigbee Alliance Website: (http://www.zigbee.org)